# Implications of the serine protease HtrA1 in amyloid precursor protein processing

Sandra Grau*, Alfonso Baldi†, Rossana Bussani‡, Xiaodan Tian§, Raluca Stefanescu§, Michael Przybylski§, Peter Richards*, Simon A. Jones*, Viji Shridhar¶, Tim Clausen‖, and Michael Ehrmann*,**

*School of Biosciences, Cardiff University, Cardiff CF10 3US, United Kingdom; †Department of Biochemistry, Section of Pathology, Second University of Naples, 80100 Naples, Italy; ‡Department of Pathology, University of Trieste, 34100 Trieste, Italy; §Department of Chemistry and Analytical Chemistry, University of Konstanz, 78457 Konstanz, Germany; ¶Department of Experimental Pathology, Mayo Clinic Cancer Center, Rochester, MN 55905; and ‖Institute for Molecular Pathology, A-1030 Vienna, Austria

Communicated by Robert Huber, Max Planck Institute for Biochemistry, Martinsried, Germany, March 8, 2005 (received for review February 8, 2005)

**The defining features of the widely conserved HtrA (high temperature requirement) family of serine proteases are the combination of a catalytic protease domain with one or more C-terminal PDZ domains and reversible zymogen activation. Even though HtrAs have previously been implicated in protein quality control and various diseases, including cancer, arthritis, and neuromuscular disorder, the biology of the human family members is not well understood. Our data suggest that HtrA1 is directly involved in the β-amyloid pathway as it degrades various fragments of amyloid precursor protein while an HtrA1 inhibitor causes accumulation of Aβ in astrocyte cell culture supernatants. Furthermore, HtrA1 colocalizes with β-amyloid deposits in human brain samples. Potential implications in Alzheimer's disease are discussed.**

protein quality control | amyloid β | C99

The HtrA (high temperature requirement) family represents a novel class of oligomeric serine proteases. Its members are classified by the combination of a catalytic domain resembling trypsin with one or more C-terminal PDZ domains. PDZ domains are protein modules that mediate specific protein–protein interactions and bind preferentially to the three to four C-terminal residues of target proteins. The N-terminal domains of HtrAs vary among the family members and include single transmembrane segments (prokaryotic DegS and human HtrA2), signal sequences, insulin-like growth factor binding domains, and serine protease inhibitor domains (human HtrA1, HtrA3, and HtrA4). Another specific feature of HtrAs is that their protease activities can be switched on and off by the novel mechanism of reversible zymogen activation (for review see refs. 1 and 2).

Prokaryotic HtrAs are involved in various stages of protein quality control such as stress sensing, activation of the unfolded protein response, and repair and degradation of misfolded proteins (3–6). Human HtrAs are believed to be involved in arthritis, apoptosis, neuromuscular disorder, and cancer although the underlying biological mechanisms are not well understood (1, 7, 8).

HtrA1 was originally identified as a gene down-regulated in simian virus 40-transformed fibroblasts (9), and recent studies indicate that HtrA1 is either absent or significantly down-regulated in various tumors (10–13). In addition, overexpression of *htrA1* inhibits proliferation and tumor growth and causes cell death (11, 12). These results suggest a tumor suppressor function for HtrA1.

Alzheimer's disease (AD) is characterized by the occurrence of various pathological features, including the formation of neurofibrillary tangles within neurons, neuronal loss, reactive gliosis, inflammation, and the accumulation of amyloid β (Aβ) in the walls of blood vessels and senile plaques (14). Aβ peptides are generated by interplay of various secretases cleaving amyloid precursor protein (APP) and C99. They accumulate in the brain and form senile plaques consisting mainly of two Aβ species, Aβ40 and Aβ42. Although Aβ peptides are continuously secreted from cells (15, 16), a metabolic balance prevents plaque formation. An imbalance in Aβ levels, caused, for example, by mutations in various AD-related genes, results in the accumulation and aggregation of these peptides (17, 18). Clearance of cerebral Aβ peptides can be achieved either by excretion into blood through the blood–brain barrier, microglia, or degradation by proteolytic enzymes (19). Recent studies have focused on neuroglial cells as important players in Aβ metabolism. Activation of astrocytes and microglia occur early in AD in the periphery of senile plaques (20). Both cell types are highly reactive to environmental changes and secrete complement proteins, inflammatory cytokines, acute phase reactants, and proteases and their inhibitors (21, 22). When astrocytes are plated on unfixed Aβ-rich brain sections from transgenic mice expressing human APP, Aβ levels decreased ≈40% within 24 h (23). Furthermore, the exposure of astrocytes to Aβ42 in cell culture supernatants led to a complete removal and degradation of Aβ within 48 h. Although these findings suggest an important role for astrocytes in Aβ metabolism it is still unclear whether Aβ digestion occurs on the cell surface of astrocytes by secreted proteases or internally. Several candidate proteases, such as insulin-degrading enzyme, neprilysin, and endothelin-converting enzyme, have been implicated in the removal of Aβ (19).

In the present article, we demonstrate that purified HtrA1 degrades various APP fragments including Aβ. Astrocytes produce significant levels of HtrA1 and Aβ, and the application of an HtrA1 inhibitor leads to accumulation of Aβ in cell culture supernatants. Consistently, HtrA1 colocalizes with amyloid deposits in human brain samples.

## Methods

**Antibodies.** Rabbit polyclonal and mouse mAbs (24) against HtrA1 were generated from purified recombinant protein (amino acids 141–480). Polyclonal and monoclonal antibodies against Aβ40, Aβ42, and β-actin were from Oncogene, Chemicon, and Santa Cruz Biotechnology, respectively. Monoclonal antibodies against APP were a gift from C. Haass (Ludwig-Maximilians-Universität, Munich).

**HtrA1 and Aβ40 ELISA.** Aβ40 levels were determined by Aβ40-specific ELISA (The Genetics Company, Zurich). HtrA1 in conditioned media was quantified by HtrA1-specific ELISA. ELISA plates were coated with monoclonal α-HtrA1 (1:100) and blocked with 5% BSA/PBS. Plates were washed with 0.05% Tween/PBS and incubated with samples for 2 h at 30°C. After washing, polyclonal α-HtrA1 (1:500) was added for 1 h at 30°C followed by a biotin- conjugated swine α-rabbit (1:5,000) (Dako

Abbreviations: AD, Alzheimer's disease; Aβ, amyloid β; APP, amyloid precursor protein; FTICR, Fourier transform ion cyclotron resonance; PS1, presenilin 1.

**To whom correspondence should be addressed. E-mail: ehrmann@cf.ac.uk.

Cytomation, Carpinteria, CA) for 1 h at 30°C. HtrA1 was detected by using horseradish peroxidase-conjugated streptavidin (1:500) (Amersham Pharmacia). Plates were developed by using 3,3′,5,5′-tetramethybenzidine (Sigma) in 100 mM citric acid and 0.1% $H_2O_2$, pH 3.95. The reaction was stopped with 7% $H_2SO_4$, and optical densities were determined at 450 nm with a plate reader (Dynex Technologies, Chantilly, VA).

**Cell Culture.** The astrocytoma cell line U373 was cultured in DMEM (Gibco) supplemented with 5% FBS in six-well plates to 80% confluence. HtrA1 inhibitor was diluted in DMEM supplemented with 0.5% FBS. Supernatants were collected 24 h after the inhibitor was added.

**Preparation of Cell Lysates.** Control and treated astrocytes were washed in PBS and lysed in STEN lysis buffer (50 mM Tris·HCl, pH 7.6/150 mM NaCl/2 mM EDTA/0.2% Nonidet P-40) for 30 min on ice. Nuclear fractions were separated by centrifugation for 10 min at 15,800 × *g* at 4°C. Protein concentration was determined with a BCA protein determination kit (Sigma).

**Recombinant Production and Purification of HtrA1.** Purified recombinant HtrA1 was produced in *Escherichia coli* (details are available in *Supporting Methods*, which is published as supporting information on the PNAS web site). Recombinant C99 and PS1 were produced as described (25). Protein samples used in protease assays contained 0.05% dodecyl maltoside. Membranes containing C99 were collected from French press lysates by ultracentrifugation using a Ti70 rotor (Beckman) at 40,000 rpm for 45 min. Membranes were washed in 50 mM Tris·HCl, pH 8.5 and 150 mM NaCl and stored at −70°C.

**Protease Assays.** Inhibition of HtrA1 by NVP-LBG976 (Novartis, Basel) was determined by preincubation of HtrA1 for 20 min at room temperature with various concentrations of inhibitor before adding the substrate. Samples were incubated at 37°C overnight in the dark. The reaction was stopped by trichloroacetic acid precipitation. After centrifugation, the supernatant (400 μl) was mixed with 600 μl of 0.5 M Tris·HCl, pH 9.5, and the absorbance was determined at 574 nm.

**MS.** For MS, protease assays using HtrA1 (90.2 nmol) and Aβ or C99 (10 nmol) as substrates were carried out in a final volume of 500 μl of 50 mM Tris·HCl, pH 8.0. After incubation at 50°C for 24 h, samples were desalted with Ziptip (Millipore) and analyzed by MALDI-TOF-MS and Fourier transform ion cyclotron resonance (FTICR)-MS.

MALDI-TOF mass spectra were obtained with a Bruker-Biflex linear time-of-flight mass spectrometer equipped with a nitrogen UV laser (337 nm) and a dual-channel plate detector (Bruker Daltonik). Two calibration standards were prepared and measured with each sample, or batch of samples, to ensure reliable mass accuracy. For proteolytic peptides measurements, a calibration mixture of bradykinin (monoisotopic $[M+H]^+$ = 1,060.57, average $[M+H]^+$ = 1,061.23), angiotensin I (monoisotopic $[M+H]^+$ = 1,296.69, average $[M+H]^+$ = 1,297.50), corticotropin (clip 18–39) (monoisotopic $[M+H]^+$ = 2,465.20, average $[M+H]^+$ = 2,466.7), and bovine insulin (average $[M+H]^+$ = 5,734.56) provided a good calibration between 500 and 6,000 Da. For the molecular mass determinations, BSA was used to calibrate over the range from 15 to 150 kDa (average $[M+3H]^{3+}$ = 22,157, $[M+2H]^{2+}$ = 33,216, $[M+H]^+$ = 66,431, and $[2M+H]^+$ = 132,861).

MALDI/electrospray ionization-FTICR-MS measurements were performed with a Bruker Apex II FTICR-MS instrument, which is equipped with an actively shielded 7-Tesla superconducting magnet, a cylindrical infinity ICR analyzer cell, and external electrospray ionization and MALDI sources with pulsed collision gas. The FTICR instrument and experimental conditions have been described (26, 27). A 100-mg·ml$^{-1}$ solution of 2,5-dihydroxybenzoic acid (Aldrich) in acetonitrile/0.1% trifluoroacetic acid in water (2:1) was used as the matrix for MALDI FTICR-MS experiments; aliquots of 0.5 μl of sample

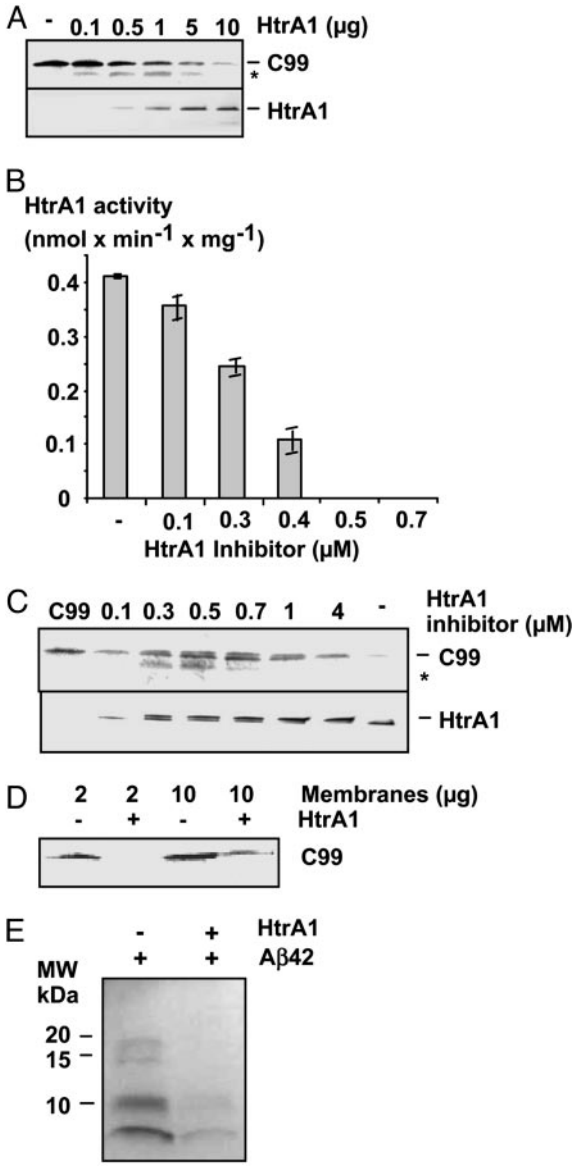


**Fig. 1.** Degradation of C99. (*A*) Purified recombinant C99 (2 μg) was incubated with increasing amounts of purified recombinant HtrA1 for 16 h at 37°C. Samples were loaded on a SDS/PAGE, immunoblotted, and stained with either monoclonal α-HtrA1 antibody or polyclonal α-C99 antiserum. The asterisk indicates a proteolytic product of C99. (*B*) To monitor the efficiency of the HtrA1 inhibitor *in vitro*, purified HtrA1 (5 μg) was preincubated for 20 min at room temperature with various inhibitor concentrations before adding 60 μg of resorufin-labeled casein. Data represent the mean of four experiments. (*C*) Purified recombinant HtrA1 (2.5 μg) was preincubated with various concentrations of HtrA1 inhibitor for 20 min before adding purified C99 (2 μg). Samples were loaded on a SDS/PAGE, immunoblotted, and stained with either monoclonal α-HtrA1 or α-C99 antibody. (*D*) Degradation of membrane-bound C99 was analyzed by using cytoplasmic membrane fractions of strain KU98 overproducing C99. Membranes were incubated with or without 10 μg of purified HtrA1. Samples were analyzed by Western blotting using α-C99 antibody. (*E*) Degradation of Aβ42. One microgram of Aβ42 (preincubated in PBS to allow multimerization) was incubated with 5 μg of HtrA1 for 14 h at 37°C. Samples were immunoblotted and stained with α-Aβ42 antibody.

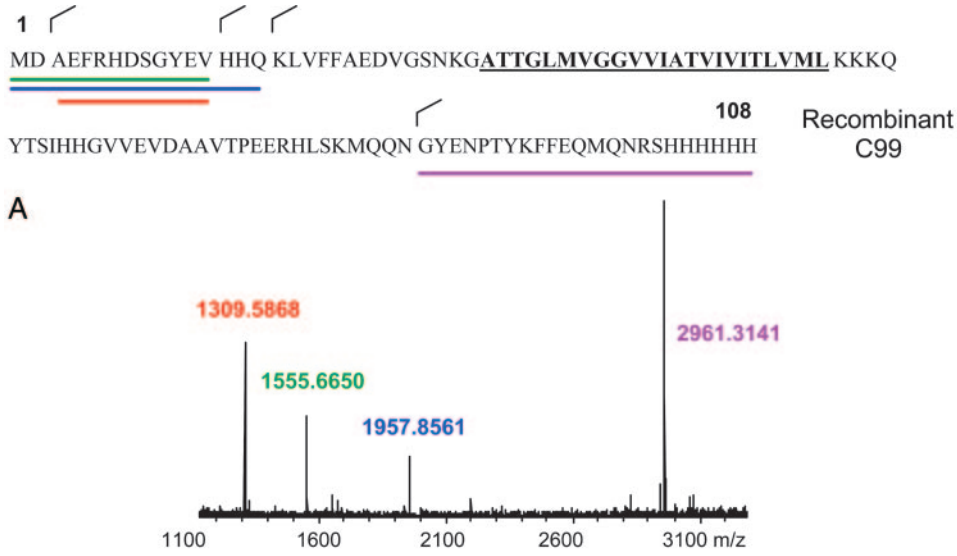


B

| Identified fragments | $[M+H]^+_{exp.}$ | $[M+H]^+_{calc.}$ | Δ $[M+H]^+$ (ppm) | Sequences |
|---|---|---|---|---|
| 3-13 | 1309.5868 | 1309.5814 | 4 | AEFRHDSGYEV |
| 1-13 | 1555.6650 | 1555.6488 | 10 | MDAEFRHDSGYEV |
| 1-16 | 1957.8561 | 1957.8252 | 16 | MDAEFRHDSGYEVHHQ |
| 86-108 | 2961.3569 | 2961.3141 | 14 | GYENPTYKFFEQMQNRSHHHHHH |

**Fig. 2.** Identification of cleavage sites of HtrA1 in C99 by MALDI-FTICR-MS. The detected cleavage sites of HtrA1 in recombinant C99 are shown. The transmembrane segment of C99 is shown in bold and underlined. Digestion was performed at an enzyme/substrate ratio of 1:50. Proteolytic fragment mixture was desalted and analyzed by MALDI-FTICR-MS as described in *Methods*. (*A*) MALDI-FTICR spectrum of HtrA1-digested C99. Monoisotopic masses were selected manually and used for fragment identification by means of the GPMAW program (Lighthouse Data, Odense, Denmark). (*B*) Fragments of C99 and sequences are identified.

and matrix solutions were mixed on the stainless-steel MALDI sample target and allowed to dry before the target was inserted; spectra were calibrated with the same calibration mixture used for MALDI-TOF-MS. The flow rate of the sample solution into the electrospray ion source was 2 $\mu$l·min$^{-1}$. Electrospray ionization conditions were ≈2 kV voltage of the nanospray needle and 100-nA spray current. Ions were accumulated for 2 s in the intermediate hexapole ion trap and then transferred into the ICR cell. A short accumulation time was used to preclude unwanted collisional activation in the hexapole. The spectra were calibrated against a commercially available mixture of peptides (Hewlett–Packard) in the 622 to 2,722 range of $m/z$ values. The experiments were performed three to five times to establish reproducibility of the results.

**Selection of Brain Samples.** Brains were collected at autopsy (University of Trieste) from 10 subjects with a well documented clinical history of AD (median age 77.2). Autopsy was performed within 36 h after death in all cases. Specimens were fixed in 10% freshly made paraformaldehyde in 0.1 M phosphate buffer and embedded in paraffin. Different sections for each specimen were processed. Light-microscopic examination was performed after staining with hematoxylin/eosin, hematoxylin/Van Gieson, Bielschowsky's silver staining, and Congo red. Morphologic analysis of tissue structure, cellular and nuclear integrity, and inflammatory infiltrates was performed.

**Immunohistochemistry.** Immunohistochemistry was carried out as described (12). Briefly, sections, embedded in paraffin, from each specimen were cut at 5–7 $\mu$m, mounted on glass, and dried overnight at 37°C. All sections were deparaffinized in xylene, rehydrated through a graded alcohol series, and washed in PBS. PBS was used for all subsequent washes and antiserum dilution. Tissue sections were heated twice in a microwave oven for 5 min each at 700 W in citrate buffer (pH 6) and then quenched sequentially in 3% hydrogen peroxide and blocked with PBS-6% nonfat dry milk (Bio-Rad) for 1 h at room temperature. Slides then were incubated at 4°C overnight with the rabbit polyclonal antiserum raised against HtrA1 (12) at a 1:10 dilution or with the mouse mAb APP amyloid-$\beta$ 1–16 (Chemicon MAB5206) at 1:25 dilution. After several washes to remove antiserum excess, the slides were incubated with diluted goat anti-rabbit or anti-mouse biotinylated antibodies (Vector Laboratories) for 1 h at room temperature. Subsequently, slides were processed by the ABC method (Vector Laboratories) for 30 min at room temperature. Diaminobenzidine and Novared (Vector Laboratories) for anti-HtrA1 and anti-APP, respectively, were used as the final chromogens, and hematoxylin was used as the nuclear counterstain. To perform double stainings, sections were first stained for anti-HtrA1 and then anti-APP. Negative controls for each tissue section were prepared by leaving out the primary antibody and with HtrA3 antibody (Abgent, San Diego).

## Results

**Native Substrates of HtrA1.** HtrA1 belongs to a novel family of oligomeric serine proteases. As only little information is available about the biological function of HtrA1 we searched for native substrates. We speculated that proteins expressed in brain might be

CELL BIOLOGY

suitable candidates as HtrA1 is significantly produced in these tissues (13). Also, HtrA2 was identified as a potential interaction partner of presenilin 1 (PS1) in a two-hybrid screen (28) and is activated by the C terminus of PS1 (29). PS1 is part of the γ-secretase complex and is involved in the formation of Aβ in AD. We therefore used purified proteins to assess whether HtrA1 could process PS1 and/or C99 *in vitro* (for information on production and purification of recombinant HtrA1 see Fig. 5, which is published as supporting information on the PNAS web site). Although HtrA1 did not process PS1, it did degrade the APP fragment C99. C99 is the precursor of the Aβ peptide and one substrate of γ-secretase. It contains 99 residues including a single transmembrane segment (see Fig. 2). To carry out protease assays *in vitro*, recombinant C99 was purified from *E. coli* (25). HtrA1 efficiently degraded C99, and one product was detected in limited proteolysis experiments (marked by an asterisk in Fig. 1).

One valuable tool for further characterization of C99 processing is an inhibitor that abolishes protease activity. NVP-LBG976, a potent inhibitor of HtrA1, was obtained from a high-throughput screen. It was active with recombinant HtrA1 as it inhibited HtrA1-dependent degradation of resorufin-labeled casein in a dose-dependent manner (Fig. 1*B*). In addition, it prevented degradation of C99 and casein at 1 and 0.5 μM concentrations, respectively (Fig. 1 *B* and *C*). The C99 processing experiments were carried out by using C99 in detergent solution, which may have contributed to the accessibility of C99 to HtrA1. We therefore repeated the protease assay by using membrane fractions containing recombinant C99, indicating that membrane-embedded C99 is degraded by HtrA1 (Fig. 1*D*). Furthermore, when Aβ42 is used as a substrate, HtrA1-dependent degradation of monomeric and multimeric forms was observed (Fig. 1*E*).

**Mass Spectrometric Identification of Cleavage Sites in C99 and Aβ.** Proteolytic digestion by HtrA1 was analyzed with C99 in comparison to Aβ(1–40), Aβ(1–42), and the cytosolic C-terminal polypeptide APP(724–770), and digestion products were identified directly by both high-resolution electrospray and MALDI-FTICR MS. All proteolytic peptide fragments were identified by molecular ions (singly and multiply charged protonated molecular ions) with mass determination accuracies of ≈10 ppm or better, which provided unequivocal assignments of partial sequences for abundant and minor fragment sequences. In addition, digestion of C99 with trypsin as a control was analyzed by FTICR-MS, yielding cleavage products at all substrate cleavage sites expected, Lys and Arg residues 6, 17, 29, 54, 55, 56, 77, 81, 93, and 101 (data not shown). A specific molecular cleavage pattern was identified for HtrA1 digestion of C99, as shown by MALDI spectrum and sequences of major product fragments (Fig. 2). Digestion was established to occur predominantly after residues Val-13, Gln-16, and Asn-85, providing degradation products of approximately equal sequence lengths. To verify these cleavage sites, Aβs and APP-C-terminal fragment γ (AICD) were used as additional substrates. The same specific cleavage sites (Val-13 and Gln-16) were also found in Aβ(1–40) and Aβ(1–42); however, additional sites were identified in Aβ(1–40) located two and three residues further downstream (see Fig. 6*A*, which is published as supporting information on the PNAS web site). A consistent molecular fragmentation pattern was found for AICD, when using APP(724–770) peptides as a substrate. Although the cleavage site at Asn-85 (or 755 when using the APP nomenclature) found in C99 was verified in APP(724–770), additional major cleavage sites were observed after Gly-734, Val-738, and His-748 residues (Fig. 6*B*). Taken together, these results show HtrA1 has no clear preference for P1 residues but generates products of similar lengths ranging between 10 and 20 residues. Because the product spectrum of the redundant substrates C99, Aβ40, and APP(724–770) is similar, further sequential or structural constraints of protein substrates seem to apply.

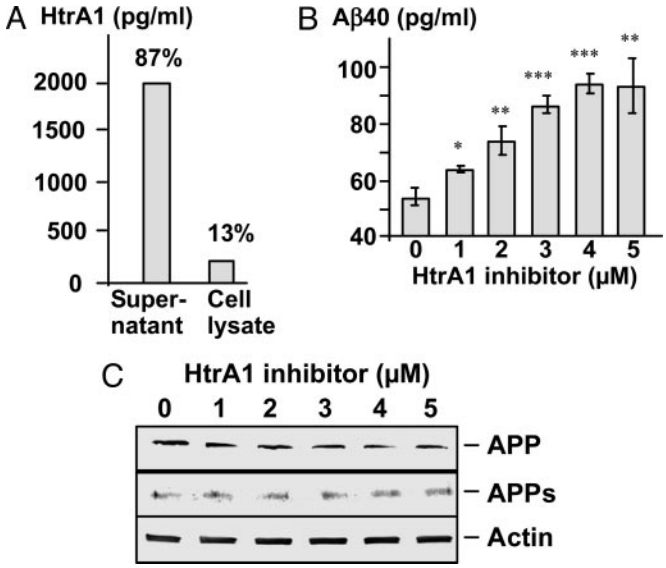


**Fig. 3.** Aβ40 accumulation in supernatants of astrocytes after HtrA1 inhibition. The astrocytoma cell line U373 was grown in six-well plates to 80% confluence in DMEM. (*A*) After 24 h, supernatants were harvested and assayed for HtrA1. (*B*) Aβ40 levels in culture supernatants were determined from cells grown with or without HtrA1 inhibitor (1–5 μM final concentration). Data represent the mean of four different treatments, each measured in duplicates. *, $P < 0.05$; **, $P < 0.01$; ***, $P < 0.001$ as determined by Student's *t* test. ELISAs in *A* and *B* were done as described in *Methods*. (*C*) Equal concentrations of protein from supernatants and cell lysates were analyzed by Western blotting to detect full-length APP, APPs, and β-actin by using antibodies against APP and β-actin, respectively.

**APP Metabolism in Astrocytes.** To obtain evidence for the physiological relevance of the *in vitro* data, we searched for a cell culture system to investigate the effects of HtrA1 on APP fragment metabolism. Recent reports suggest that neuroglial cells, mainly astrocytes, participate in Aβ metabolism (23, 30). The human astrocytoma cell line U373 produces and secretes HtrA1 (1,900 pg/ml in 24 h) as determined by an HtrA1-specific ELISA (Fig. 3*A*). Furthermore, astrocytes secrete Aβ40 (55 pg/ml in 24 h) as measured in an Aβ40-specific ELISA (Fig. 3*B*), and APP levels can be visualized on Western blots (Fig. 3*C*), making this untransfected cell line a suitable system for investigating the role of HtrA1 in APP/C99/Aβ metabolism. Because of the unavailability of specific ELISAs to quantify C99 levels and the known instability of AICD (31), Aβ40 accumulation was investigated in the presence and absence of HtrA1 inhibitor.

The application of HtrA1 inhibitor resulted in a significant dose-dependent increase in Aβ40 accumulation in cell culture supernatants (Fig. 3*B*). Western blot experiments of the same supernatants indicated that the accumulation was not caused by an increase in APP levels (Fig. 3*C*) or β-secretase processing as detected by monitoring the soluble APP-β fragment (APPs) (Fig. 3*C*). In addition, Western blot analysis of corresponding cell lysates using an antibody against β-actin confirmed that equal amounts of total protein and cells were used (Fig. 3*C*). Previous studies showed that the HtrA1 inhibitor is not active against trypsin but decreases thrombin and chymotrypsin activity to 75% and 10% at 1 μM concentration, respectively (data not shown). We therefore used two different approaches to confirm the specificity of our results. Inhibition of the bacterial HtrA1 homologue DegP was examined by using resorufin-labeled casein as substrate. Even a high inhibitor concentration (5 μM) did

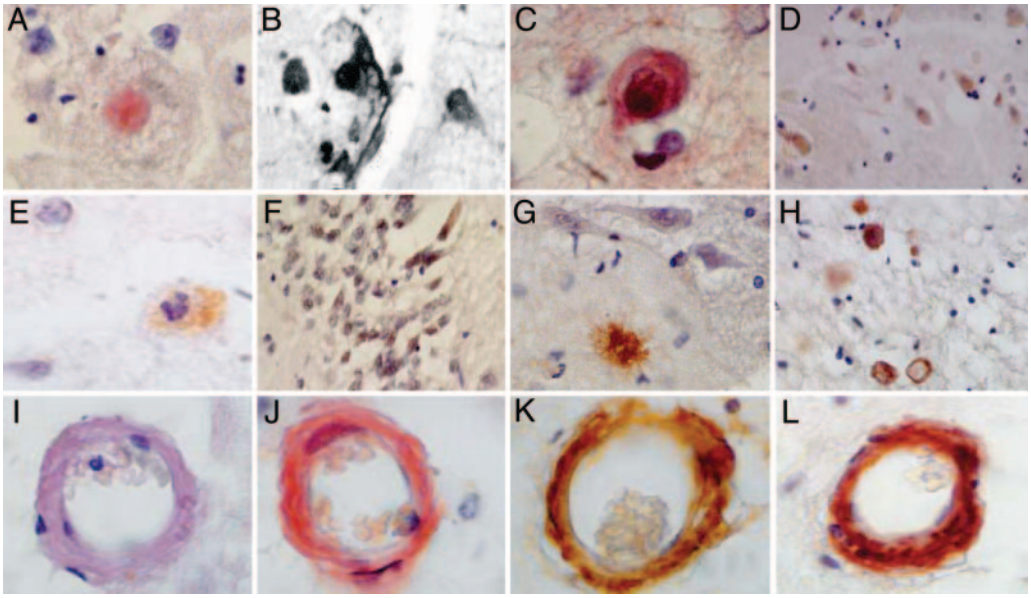


**Fig. 4.** Histopathological and immunohistochemical analysis of AD's autoptic brains. For histopathological analysis, AD brains were analyzed by hematoxylin/eosin staining, Bielschowsky's silver staining, and Congo red staining. (*A–C*) Typical lesions shown are: an amyloid plaque positive for Congo red staining (*A*); a neurofibrillar tangle evidenced by Bielschowsky's silver staining (*B*); and a dystrophic neuron positive for β-amyloid immunohistochemistry (*C*). (*D–F*) Analysis of HtrA1 expression by immunohistochemistry revealed that the protein was present both in cortical neurons (*D* and *F*) and astrocytes (*E*). (*G–L*) For colocalization of HtrA1 and amyloid deposits, HtrA1 was expressed in the brain's areas where amyloid deposits were evident, such as in amyloid plaques (*G*), dystrophic neurons (*H*), or peri-vascular level (*I–L*). The same small arteriole of a cortical region evidenced by hematoxylin/eosin (*I*) is positive for Congo red staining (*J*), HtrA1 (*K*), and β-amyloid immunohistochemistry (*L*). (Magnifications: ×500, *A*, *B*, *D*, *E*, and *G-L*; ×1,000, *C* and *F*.)

not have any effect on DegP activity, which was 0.56 nmol casein $\times$ $min^{-1}$ $\times$ $mg^{-1}$ HtrA1 with or without inhibitor. Also, a broad range protease inhibitor mixture (Calbiochem) acting against all major proteases, including thrombin and chymotrypsin, was used in the cell culture system, and no increase in Aβ levels was observed (data not shown). These results support the model that HtrA1 is a candidate modulator of Aβ levels.

**Colocalization of HtrA1 and Amyloid Deposits in Human Brain Samples.** Neuropathological investigation of brains from AD patients by hematoxylin/eosin staining, Congo red staining, Bielschowsky's silver staining, and β-amyloid immunohistochemistry revealed the presence of the characteristic lesions in this disease, such as Aβ amyloid plaques, dystrophic neurons, neurofibrillary tangles, and perivascular amyloid (Fig. 4 *A–C*). By using a specific antiserum, we investigated the expression of HtrA1 in these samples. The specificity of the HtrA1 antiserum and its suitability for immunohistochemistry was previously validated, including the observation that it does not crossreact with HtrA2 and HtrA3 (32). In agreement with the above results, HtrA1 was strongly expressed in astrocytes and cortical neurons (Fig. 4 *D–F*). In contrast, HtrA1 expression in neuroglial components and neurons of normal adult brains is always very low (33). HtrA1 also colocalizes with β-amyloid deposits in human brain samples. In fact, most amyloid plaques, positively stained with Congo red, were also positive for HtrA1 expression (Fig. 4*G*). Moreover, several dystrophic neurons, positive for β-amyloid immunohistochemistry, stained positive also for HtrA1 (Fig. 4*H*). This colocalization was also evident at the perivascular level as shown in consecutive sections of a representative small arteriole in the hippocampus by staining with hematoxylin/eosin, Congo red, β-amyloid, and HtrA1 immunohistochemistry (Fig. 4 *I–L*).

## Discussion

We describe a role of HtrA1, a member of the widely conserved HtrA family of serine proteases, in alternative proteolytic processing of APP fragments. With respect to C99 metabolism, HtrA1 represents a candidate protease that processes C99 in addition to γ-secretase in the plasma membrane. With respect to Aβ degradation, HtrA1 could function in concert with other proteases such as insulin-degrading enzyme and neprilysin that cleave Aβ (19).

The presence of secreted and intracellular HtrA1 suggests that HtrA1 has the potential to cleave the extracellular and intracellular segments of C99. This notion is supported by mass spectrometric mapping of the cleavage sites. These sites were Val-13 and Gln-16 in the extracellular segment and Asn-85 in the intracellular segment. Val-13 and Gln-16 are located one and four residues upstream of the α-secretase cleavage site, respectively (34). Further processing of these HtrA1 products is expected as the slightly shorter product of α-secretase is a substrate of γ-secretase (35). As the resulting p3 fragment is nonpathogenic, it can be expected that the potentially further processed HtrA1 products are also nonpathogenic.

MS detected a similar pattern of cleavage sites in Aβ40, Aβ42, and AICD, and degradation of the pathogenic Aβ42 peptide was confirmed by *in vitro* proteolysis experiments. HtrA1 activity could therefore reduce formation of Aβ deposits in human brains by competing with γ-secretase for substrate and removing Aβ. The finding that HtrA1 interferes with Aβ production at least in astrocytes supports this model. Here, the application of an HtrA1 inhibitor led to a significant accumulation of Aβ in cell culture supernatants.

Furthermore, immunohistochemistry indicated a striking colocalization of HtrA1 with amyloid deposits and APP in blood vessels and neurons of AD patients. HtrA1 was strongly expressed in astrocytes and cortical neurons (Fig. 4 *D–F*), whereas expression in neuroglial components and neurons of normal adult brains is always very low (33). In particular, the percentage of neurons overexpressing HtrA1 ranged from 1–2% of cerebellum and occipital cortex to 2–4% of frontal, parietal, and temporal cortex and 8–10% of hippocampus.

Most of the well studied HtrA family members play important roles in protein quality control (1, 2). In analogy, it might be this

function that is responsible for the HtrA1-dependent removal of several APP fragments that are produced by the various secretases. This model is supported by recent reports indicating that other quality-control elements interact with amyloid deposits, are modulating protein aggregation in poly Gln diseases, and can suppress toxicity (36). These results suggest that activation of protein quality-control factors represents one promising general strategy for tackling degenerative diseases that are based on protein aggregation and amyloid formation.

Future studies should aim at identifying conditions that activate HtrA1 in brain tissue, either on the genetic or enzymatic level, and investigating the effect of activation on A$\beta$ levels and plaque formation in an animal model of AD. The mechanism of transcriptional activation of HtrA1 is currently unknown but activation of protease activity by peptides binding to its PDZ domain has been reported (37). This mechanism of reversible zymogen activation appears to be conserved in HtrA family as it has also been observed for human HtrA2 and prokaryotic DegS and DegP (5, 6, 29, 38, 39).

We thank Novartis for providing HtrA1 inhibitor, Harald Steiner (Ludwig-Maximilians-Universität, Munich) for materials and discussions, Phillipe Gasque (Cardiff University) for neuronal cell lines, and David Farley and Bob Crowl for discussions. This work was supported by FUTURA-ONLUS (A.B.) and Deutsche Forschungsgemeinschaft (M.P.).

1. Clausen, T., Southan, C. & Ehrmann, M. (2002) *Mol. Cell* **10,** 443–455.
2. Ehrmann, M. & Clausen, T. (2004) *Annu. Rev. Genet.* **38,** 709–724.
3. Spiess, C., Beil, A. & Ehrmann, M. (1999) *Cell* **97,** 339–347.
4. Krojer, T., Garrido-Franco, M., Huber, R., Ehrmann, M. & Clausen, T. (2002) *Nature* **416,** 455–459.
5. Walsh, N. P., Alba, B. M., Bose, B., Gross, C. A. & Sauer, R. T. (2003) *Cell* **113,** 61–71.
6. Wilken, C., Kitzing, K., Kurzbauer, R., Ehrmann, M. & Clausen, T. (2004) *Cell* **117,** 483–494.
7. Jones, J. M., Datta, P., Srinivasula, S. M., Ji, W., Gupta, S., Zhang, Z., Davies, E., Hajnoczky, G., Saunders, T. L., Van Keuren, M. L., *et al*. (2003) *Nature* **425,** 721–727.
8. Suzuki, Y., Takahashi-Niki, K., Akagi, T., Hashikawa, T. & Takahashi, R. (2004) *Cell Death Differ.* **11,** 208–216.
9. Zumbrunn, J. & Trueb, B. (1996) *FEBS Lett.* **398,** 187–192.
10. Shridhar, V., Sen, A., Chien, J., Staub, J., Avula, R., Kovats, S., Lee, J., Lillie, J. & Smith, D. I. (2002) *Cancer Res.* **62,** 262–270.
11. Chien, J., Staub, J., Hu, S. I., Erickson-Johnson, M. R., Couch, F. J., Smith, D. I., Crowl, R. M., Kaufmann, S. H. & Shridhar, V. (2004) *Oncogene* **23,** 1636–1644.
12. Baldi, A., De Luca, A., Morini, M., Battista, T., Felsani, A., Baldi, F., Catricalà, C., Amantea, A., Noonan, D. M., Albini, A., *et al*. (2002) *Oncogene* **21,** 6684–6688.
13. Nie, G.-Y., Hampton, A., Li, Y., Findlay, J. & Salamonsen, L. (2003) *Biochem. J.* **371,** 39–48.
14. Selkoe, D. J. (2001) *Physiol. Rev.* **81,** 741–766.
15. Haass, C., Schlossmacher, M. G., Hung, A. Y., Vigo-Pelfrey, C., Mellon, A., Ostaszewski, B. L., Lieberburg, I., Koo, E. H., Schenk, D., Teplow, D. B., *et al*. (1992) *Nature* **359,** 322–325.
16. Seubert, P., Oltersdorf, T., Lee, M. G., Barbour, R., Blomquist, C., Davis, D. L., Bryant, K., Fritz, L. C., Galasko, D., Thal, L. J., *et al*. (1993) *Nature* **361,** 260–263.
17. Czech, C., Tremp, G. & Pradier, L. (2000) *Prog. Neurobiol.* **60,** 363–384.
18. Hutton, M. & Hardy, J. (1997) *Hum. Mol. Genet.* **6,** 1639–1646.
19. Tanzi, R. E., Moir, R. D. & Wagner, S. L. (2004) *Neuron* **43,** 605–608.
20. Nagele, R. G., Wegiel, J., Venkataraman, V., Imaki, H. & Wang, K. C. (2004) *Neurobiol. Aging* **25,** 663–674.
21. von Bernhardi, R. & Ramirez, G. (2001) *Biol. Res.* **34,** 123–128.
22. Lafon-Cazal, M., Adjali, O., Galeotti, N., Poncet, J., Jouin, P., Homburger, V., Bockaert, J. & Marin, P. (2003) *J. Biol. Chem.* **278,** 24438–24448.
23. Wyss-Coray, T., Loike, J. D., Brionne, T. C., Lu, E., Anankov, R., Yan, F., Silverstein, S. C. & Husemann, J. (2003) *Nat. Med.* **9,** 453–457.
24. Caterson, B., Christner, J. E. & Baker, J. R. (1983) *J. Biol. Chem.* **258,** 8848–8854.
25. Harnasch, M., Grau, S., Dove, S., Hochschild, N., Iskandar, M.-K., Xia, W. & Ehrmann, M. (2004) *Mol. Membr. Biol.* **21,** 373–383.
26. Damoc, E., Youhnovski, N., Crettaz, D., Tissot, J. D. & Przybylski, M. (2003) *Proteomics* **3,** 1425–1433.
27. Rossier, J. S., Youhnovski, N., Lion, N., Damoc, E., Becker, S., Reymond, F., Girault, H. H. & Przybylski, M. (2003) *Angew. Chem. Int. Ed. Engl.* **42,** 54–58.
28. Gray, C. W., Ward, R. V., Karran, E., Turconi, S., Rowles, A., Viglienghi, D., Southan, C., Barton, A., Fantom, K. G., West, A., *et al*. (2000) *Eur. J. Biochem.* **267,** 5699–5710.
29. Gupta, S., Singh, R., Datta, P., Zhang, Z., Orr, C., Lu, Z., DuBois, G., Zervos, A. S., Meisler, M. H., Srinivasula, S. M., *et al*. (2004) *J. Biol. Chem.* **279,** 45844–45854.
30. Guenette, S. Y. (2003) *Trends Mol. Med.* **9,** 279–280.
31. Chang, Y., Tesco, G., Jeong, W. J., Lindsley, L., Eckman, E. A., Eckman, C. B., Tanzi, R. E. & Guenette, S. Y. (2003) *J. Biol. Chem.* **278,** 51100–51107.
32. De Luca, A., De Falco, M., De Luca, L., Penta, R., Shridhar, V., Baldi, F., Campioni, M., Paggi, M. G. & Baldi, A. (2004) *J. Histochem. Cytochem.* **52,** 1609–1617.
33. De Luca, A., De Falco, M., Severino, A., Campioni, M., Santini, D., Baldi, F., Paggi, M. G. & Baldi, A. (2003) *J. Histochem. Cytochem.* **51,** 1279–1284.
34. Esch, F. S., Keim, P. S., Beattie, E. C., Blacher, R. W., Culwell, A. R., Oltersdorf, T., McClure, D. & Ward, P. J. (1990) *Science* **248,** 1122–1124.
35. Haass, C., Hung, A. Y., Schlossmacher, M. G., Teplow, D. B. & Selkoe, D. J. (1993) *J. Biol. Chem.* **268,** 3021–3024.
36. Barral, J. M., Broadley, S. A., Schaffar, G. & Hartl, F. U. (2004) *Semin. Cell Dev. Biol.* **15,** 17–29.
37. Murwantoko, Yano, M., Ueta, Y., Murasaki, A., Kanda, H., Oka, C. & Kawaichi, M. (2004) *Biochem. J.* **381,** 895–904.
38. Martins, L. M., Turk, B. E., Cowling, V., Borg, A., Jarrell, E. T., Cantley, L. C. & Downward, J. (2003) *J. Biol. Chem.* **278,** 49417–49427.
39. Jones, C. H., Dexter, P., Evans, A. K., Liu, C., Hultgren, S. J. & Hruby, D. E. (2002) *J. Bacteriol.* **184,** 5762–5771.